NANO LETTERS

2008
Vol. 8, No. 3
872-875

A Radio Frequency Single-Electron Transistor Based on an InAs/InP Heterostructure Nanowire

Henrik A. Nilsson,*,† Tim Duty,‖ Simon Abay,§ Chris Wilson,§ Jakob B. Wagner,‡ Claes Thelander,† Per Delsing,§ and Lars Samuelson†

Solid State Physics, Lund University, Box 118, S-221 00, Lund, Sweden, Microtechnology and Nanoscience, Chalmers University of Technology, S-412 96, Göteborg, Sweden, School of Physical Sciences, The University of Queensland, St. Lucia, 4072 Australia, and Polymer and Materials Chemistry/nCHREM, Lund University, Box 124, S-221 00, Lund, Sweden

Received November 28, 2007; Revised Manuscript Received January 23, 2008

ABSTRACT

We demonstrate radio frequency single-electron transistors fabricated from epitaxially grown InAs/InP heterostructure nanowires. Two sets of double-barrier wires with different barrier thicknesses were grown. The wires were suspended 15 nm above a metal gate electrode. Electrical measurements on a high-resistance nanowire showed regularly spaced Coulomb oscillations at a gate voltage from −0.5 to at least 1.8 V. The charge sensitivity was measured to 32 μe_{rms} $Hz^{-1/2}$ at 1.5 K. A low-resistance single-electron transistor showed regularly spaced oscillations only in a small gate-voltage region just before carrier depletion. This device had a charge sensitivity of 2.5 μe_{rms} $Hz^{-1/2}$. At low frequencies this device showed a typical 1/*f* noise behavior, with a level extrapolated to 300 μe_{rms} $Hz^{-1/2}$ at 10 Hz.

Single-electron transistors[1] (SETs) are extremely sensitive electrometers. In the so-called RF-SET[2] the dissipation in the SET is measured using radio frequency (rf) reflectometry which extends the operation frequency by several orders of magnitude to well above 10 MHz. This has allowed operation at frequencies above the 1/*f* noise corner,[3] which has resulted in very high sensitivities.[4,5] Even higher frequencies can be reached by using the RF-SET as a mixer.[6,7] The combination of high speed and very high charge sensitivity has made it possible to study a wide range of physical phenomena such as nanomechanical oscillators,[8,9] charge fluctuators,[10–12] discrete electron transport,[13–15] and qubit readout.[16–18] So far most RF-SETs have been using Al/AlO_x/Al tunnel junctions; however, SETs based on GaAs quantum dots[10,15] and carbon nanotubes[19] have also been used in the rf mode.

Recent technological developments have allowed us to fabricate a new type of SET based on epitaxially grown InAs/InP heterostructure nanowires.[20,21] The difference in band gap between InAs and InP can be used to form tunnel barriers, and the SET structure can be grown vertically in the nanowire. These nanowire SETs have several unique properties which may offer enhanced electrometer performance. First, the charging energy of the nanowire SETs can be very high, since the size of the middle island between the two tunnel barriers can be defined by epitaxial growth. Second, the very high quality of the heterostructure interfaces results in very uniform and epitaxial tunnel barriers. Another interesting property is that the nanowire SETs can easily be suspended above a substrate.

In this paper we present the first demonstration of a nanowire SET operated in the rf mode. We demonstrate operation at 1.5 K, and we obtain a charge sensitivity close to that of the best aluminum RF-SETs.[4] In addition we present low-frequency noise measurements of this nanowire RF-SET.

Two batches of InAs/InP nanowires with diameters of 50–60 nm were grown by chemical beam epitaxy from Au aerosol nanoparticles.[22,23] In the middle of the 2–3 μm long InAs wires, two InP barriers were grown. In the first batch of wires the barriers were grown approximately 4–5 nm thick with a spacing of 150 nm. This double-barrier structure is shown in Figure 1a. In the second batch, the barriers were grown thinner, 2–3 nm, with a spacing of 50 nm. The two batches of wires will be referred to as the high resistance (first batch) and the low resistance wires (second batch).

To measure the nanowires, metal stripe structures were made by electron beam lithography and Ti/Au evaporation/lift-off on low-doped Si substrates that were capped with

* Corresponding author. E-mail: henrik.nilsson@ftf.lth.se.
† Solid State Physics, Lund University.
‡ Polymer and Materials Chemistry/nCHREM, Lund University.
§ Microtechnology and Nanoscience, Chalmers University of Technology.
‖ School of Physical Sciences, The University of Queensland.

10.1021/nl0731062 CCC: $40.75
Published on Web 02/27/2008

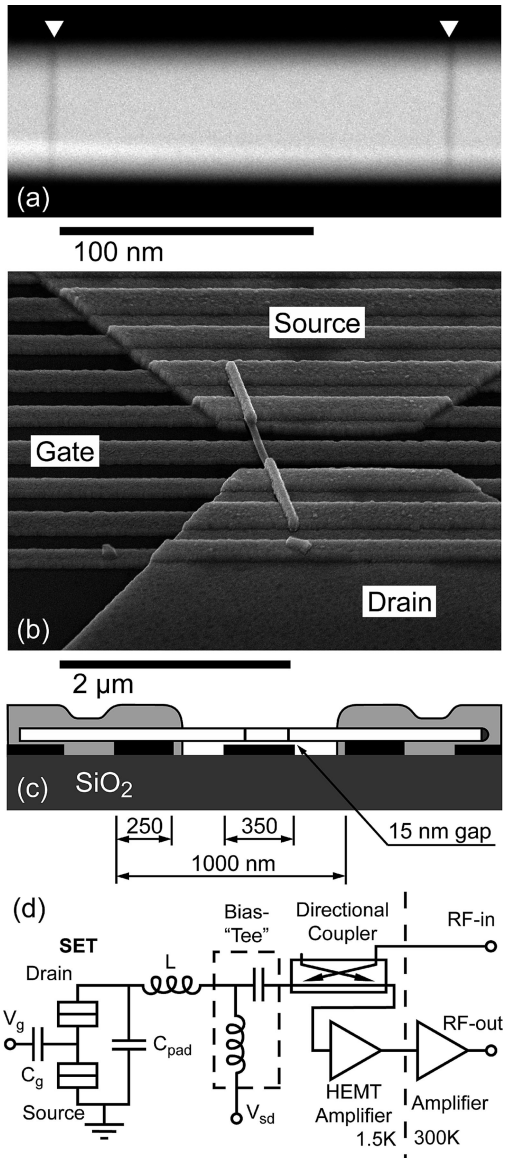

Figure 1. (a) High angle annular dark-field scanning TEM image of two 4–5 nm InP barriers grown with a spacing of 150 nm in an InAs nanowire. (b) Scanning electron microscope image of an electrically contacted nanowire suspended over a metal gate strip. (c) Schematic of the suspended nanowire. The gap between the nanowire and the gate strip is 15 nm. (d) Schematic of the measurement setup, both for radio frequency and for direct current. Filters are not shown.

500 nm SiO_2. Arrays of 250 nm wide and 65 nm high source−drain stripes with a length of 16 μm and a spacing of 1 μm were first made on the substrates. After this, 350 nm wide and 50 nm high gate stripes with a length of 18 μm were made in between the previous ones; see Figure 1b. A height difference of 15 nm between the two interdigitated arrays was verified with an atomic force microscope. Finally 100 nm thick bond pads were made by optical lithography, Ti/Au evaporation, and lift-off.

The nanowires were transferred mechanically to the metal stripe substrates. Wires lying perpendicular to the metal stripes and centered over a gate stripe were located using a scanning electron microscope. Ohmic contacts were made to the nanowires and the gate stripes by electron beam lithography and Ni/Au evaporation and liftoff. For details on preparation of contacts to InAs nanowires, see ref 24. An example of a suspended nanowire SET can be seen in Figure 1b, and a schematic side view is shown in Figure 1c.

The electrical measurements were performed in a He^4 cryostat, with the possibility to pump to 1.5 K. A schematic of our measurement setup can be seen in Figure 1d. The high impedance of the nanowire SET was transformed to a lower value by an LC resonant circuit. The source of the SET was grounded, and the drain was connected by a bonding wire to a printed circuit board inductor. The resonator capacitance is formed by the stray capacitance of the bond pad. A monochromatic high-frequency signal, the carrier f_c, was coupled on to the line toward the sample by a directional coupler. The rf carrier line was attenuated both at room temperature and in the He^4 bath. After reflection at the resonant circuit, the signal was fed into a HEMT-based low noise amplifier with an input impedance of 50 Ω, submerged in the pumped He^4 bath. The reflected rf signal was amplified by an additional amplifier at room temperature. A dc source−drain voltage could be introduced by a bias tee. This also made it possible to independently measure the dc current through the SET. The SET gate was connected directly to a low-frequency line. Both drain and gate lines were filtered at low temperature by lumped element low-pass filters as well as powder filters.

To record the SET stability diagrams, the reflected rf signal was mixed together with the carrier signal (homodyne mixing) at room temperature. The signal from the mixer was low-pass filtered and recorded by an oscilloscope. When sweeping the gate of the SET and stepping the source−drain bias the amplitude of the reflected carrier was measured. Due to a thermal offset of several millivolts, it was difficult to directly determine the exact value of the source−drain dc bias; however the zero bias point could be extracted from the symmetry of the stability diagram.

In order to measure the sensitivity of the RF-SET, a small voltage modulation, with frequency f, was applied to the gate. The rf signal from the room temperature amplifier was now fed directly into an Advantest R3131 spectrum analyzer. The RF-SET amplitude modulated the signal and on the spectrum analyzer the sidebands $f_c - f$ and $f_c + f$ appeared together with the carrier f_c. The sensitivity was deduced from the signal-to-noise ratio of one of the sidebands, see ref 4.

For the low-frequency noise measurement the rf signal was again mixed down by homodyne mixing and measured by a Stanford SR785 dynamic signal analyzer. A small modulation signal was applied to the gate for calibration of the data in units of e_{rms} $Hz^{-1/2}$.

From $I-V$ curves at low bias, the resistance of the high-resistance SET was measured to 600 kΩ at 4.2 K. This device showed regularly spaced Coulomb oscillations in gate voltage from approximately −0.5 V up to at least 1.8 V. A measurement of the dc current, through the SET as a function of gate voltage at low source–drain bias, can be found in Figure 2. For this device the LC circuit had a resonance frequency of 499 MHz. Here we used a

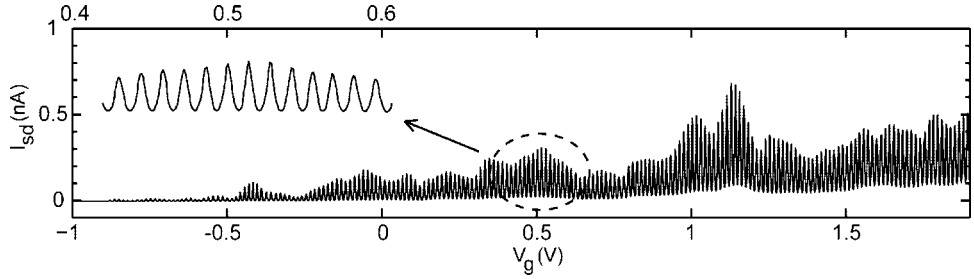

Figure 2. Measurement on the high-resistance wire at $T = 4.2$ K. Direct current through the SET as a function of V_g at low V_{sd}. As can be seen there are no charge rearrangements during this sweep.

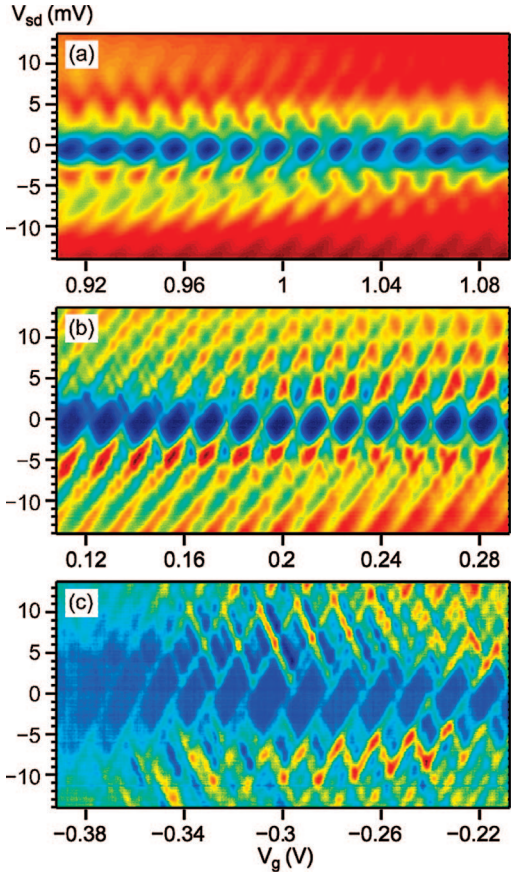

Figure 3. Measurements on the high-resistance wire at $T = 1.5$ K. Reflection of the 499 MHz carrier at the RF-SET for various V_{sd} and V_g. The V_{sd} scale is corrected for a thermal offset voltage so that the diamonds are centered on $V_{sd} = 0$ V. (a) At high V_g, the diamonds are slightly rounded. (b) At low positive V_g, the diamonds are sharp. (c) At negative V_g, the wire is depleted from carriers and the diamonds start to disappear.

450 MHz HEMT-amplifier, with a noise temperature of 2.5 K. The reflected rf signal as a function of V_{sd} and V_g can be found in Figure 3. At high V_g, see Figure 3a, the rf Coulomb diamonds have slightly rounded corners. This is because the applied voltage is not negligible compared to the height of the tunnel barriers, and therefore the effective height of the barriers is decreased. At a small positive V_g, Figure 3b, the Coulomb diamonds are sharp and a rich structure can be seen also at higher V_{sd}. At some negative V_g the nanowire becomes depleted of electrons and the stability diagram begins to break up; see Figure 3c. The limit of depleting the nanowire can also be seen in the dc gate sweep in Figure 2. The charging energy, E_c, was 1.2 meV, corresponding to 14 K or a total SET-island capacitance, C_Σ, of 69 aF. The Coulomb oscillation period was 15 mV, corresponding to a gate capacitance, C_g, of 11 aF. A calculation using the cylinder-on-plate model[25] and $\epsilon_r = 1.05$ for LHe, gives a gate capacitance of 9 aF. The plate capacitor model, with $\epsilon_r = 11.8$ for InP, gives a junction capacitance of 55 aF. This gives a sum capacitance, $C_\Sigma = 119$ aF, which is approximately two times larger than the measured one. However, the plate capacitor model has been observed to give two to three times too large junction capacitance in a similar device, see ref 21. During the whole dc gate sweep, from -1 to $+1.8$ V, no background charge rearrangements could be seen. The charge sensitivity of the high resistive RF-SET was however quite low. A signal-to-noise ratio, SNR, of 18 dB was measured using a 63 me_{rms} signal and a resolution bandwidth, RBW, of 30 kHz, giving a charge sensitivity of 32 μe_{rms} $Hz^{-1/2}$.

For the low-resistance wires no $I-V$ curves were recorded but an approximate resistance value of 65 kΩ was measured. Here the LC circuit had a resonance frequency of 367.5 MHz and a Q value of 6.9. A 350 MHz HEMT amplifier was used, also with a noise temperature of 2.5 K. The area in gate voltage with reproducible oscillations was small, only from -0.2 to -0.1 V; see Figure 4a. We believe that this is caused by lowering of the bandgap in the InP barriers due to the strain from the InAs. Changes of the electronic properties of thin InP segment in InAs are suggested in ref 26. The charging energy, E_c, of this device was 1.0 meV, corresponding to 11 K or a C_Σ of 80 aF. The oscillation period was 40.7 mV, corresponding to a gate coupling capacitance, C_g, of 3.9 aF. The weaker gate coupling compared to the high-resistance sample is due to the smaller island of the low resistance wires, and/or that the island is not completely centered above the gate strip. The cylinder-on-plate model gives a calculated gate capacitance of 3 aF and the plate capacitor model gives a junction capacitance of 100 aF. This gives a sum capacitance, $C_\Sigma = 203$ aF, again a factor of 2−3 larger than the measured value.

The RF-SET was biased at the slope of the Coulomb peak at $V_g = -0.155$ V; see Figure 4a. Here the SNR was measured to be 23.4 dB using a 2.9 me_{rms} gate modulation signal and a RBW of 3 kHz. The rf power at the tank circuit was −72.7 dBm. This gives a charge sensitivity of 2.5 μe_{rms} $Hz^{-1/2}$, which is comparable to the best Al/AlO_x RF-SET

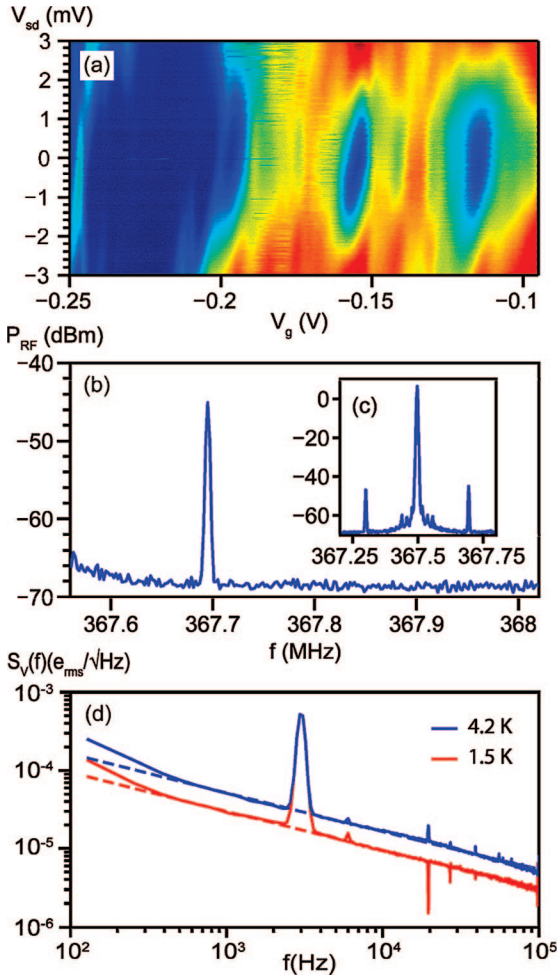

Figure 4. Measurements on the low resistance wires at $T = 1.5$ K. (a) Reflection of the 367.5 MHz carrier at the RF-SET for various V_{sd} and V_g. (b, c) Spectrum from the RF-SET using a 2.9 me_{rms} gate signal and a RBW of 3 kHz. Biased at the slope of the Coulomb peak at $V_g = -0.155$ V. (d) Low-frequency noise at both 1.5 and 4.2 K, with a 5.9 me_{rms} signal at 2.9 kHz applied to the gate. Biased at the slope of the Coulomb peak at $V_g = -0.155$ V. The dashed lines indicate 1/*f* slopes.

results; see ref 4. The data recorded by the spectrum analyzer can be found in panels b and c of Figure 4.

The substantially better charge sensitivity in this sample compared to the high resistive sample we attribute to the large difference in resistance. The low resistive sample is close to optimally matched, whereas the high resistive sample is poorly matched to the tank circuit resulting in a very small carrier modulation and consequently a substantially lower charge sensitivity.

A noise spectrum from the low-resistance device biased at the steep slope of the Coulomb peak at $V_g = -0.155$ V and applying a 5.9 me_{rms} signal at 2.9 kHz, can be seen in Figure 4d. The amplifier noise is subtracted. The noise showed typical 1/*f* behavior both at 1.5 and at 4.2 K. The level of 1/*f* noise at 10 Hz is extrapolated to 300 μe_{rms} $Hz^{-1/2}$ at 1.5 K and 500 μe_{rms} $Hz^{-1/2}$ at 4.2 K. It is somewhat surprising that this sample shows 1/*f* noise which is very similar to aluminum SETs despite the different material, the epitaxial tunnel barriers, and the fact that the SET is suspended above the substrate. Since the wire is suspended above the substrate, the 1/*f* noise should come from the wire itself rather than from the substrate. Above 1 MHz the noise was dominated by the cold amplifier.

In conclusion, we have demonstrated RF-SETs made from suspended epitaxially grown InAs/InP heterostructure nanowires. Two sets of wires were grown, one with 600 kΩ resistance and one with a resistance of 65 kΩ. The high resistance SETs showed Coulomb oscillations from −0.5 V up to at least 1.8 V. The low resistance SETs showed few Coulomb oscillations just above depletion of carriers. This device had a charge sensitivity of 2.5 μe_{rms} $Hz^{-1/2}$ at 1.5 K. At low frequencies, it showed a typical 1/*f* behavior.

Acknowledgment. This work was supported by the Swedish Foundation for Strategic Research (SSF), the Swedish Research Council (VR), the Knut and Alice Wallenberg Foundation, the Office of Naval Research (ONR), and the EU program NODE 015783.

References

(1) Likharev, K. K. *IEEE Trans. Magn.* **1987**, *MAG-23*, 1142.
(2) Schoelkopf, R. J.; Wahlgren, P.; Kozhevnikov, A. A. *Science* **1998**, *280*, 1238.
(3) Zimmerli, G.; Eiles, T. M.; Kautz, R. L. *Appl. Phys. Lett.* **1992**, *61*, 237.
(4) Brenning, H. T. A.; Kafanov, S.; Kubatkin, S. *J. Appl. Phys.* **2006**, *100*, 114321.
(5) Buehler, T. M.; Reilly, D. J.; Starrett, R. P. *J. Appl. Phys.* **2004**, *96*, 4508.
(6) Swenson, L. J.; Schmidt, D. R.; Aldridge, J. S. *Appl. Phys. Lett.* **2005**, *86*, 173112.
(7) Reilly, D. J.; Buehler, T. M. *Appl. Phys. Lett.* **2005**, *87*, 163122.
(8) Knobel, G.; Cleland, A. N. *Nature* **2003**, *424*, 291.
(9) LaHaye, D.; Buu, O.; Camarota, B. *Science* **2004**, *304*, 74.
(10) Fujisawa, T.; Hirayama, Y. *Appl. Phys. Lett.* **2000**, *77*.
(11) Aumentado, J.; Keller, M. W.; Martinis, J. M. *Phys. Rev. Lett.* **2004**, *92*, 066802.
(12) Court, N. A.; Ferguson, A. J.; Lutchyn, R.; Clark, R. G. A quantitative study of quasiparticle traps usion the single-Cooper-pair-transistor. *arXiv:0710.2760 [cond-mat.supr-con]*, 2007.
(13) Lu, W.; Ji, Z. Q.; Pfeiffer, L. *Nature* **2003**, *423*, 422.
(14) Bylander, J.; Duty, T.; Delsing, P. *Nature* **2005**, *434*, 361.
(15) Fujisawa, T.; Hayashi, T.; Tomita, R. *Science* **2006**, *312*, 1634.
(16) Lehnert, K. W.; Bladh, K.; Spietz, L. F. *Phys. Rev. Lett.* **2003**, *90*, 027002.
(17) Duty, T.; Gunnarsson, D.; Bladh, K. *Phys. Rev. B* **2004**, *69*, 140503(R).
(18) Guillaume, A.; Schneiderman, J. F.; Delsing, P. *Phys. Rev. B* **2004**, *69*.
(19) Roschier, L.; Sillanpaa, M.; Wang, T. H. *J. Low Temp. Phys.* **2004**, *136*, 465.
(20) Bjork, M. T.; Ohlsson, B. J.; Sass, T. *Appl. Phys. Lett.* **2002**, *80*, 1058.
(21) Thelander, C.; Martensson, T.; Bjork, M. T. *Appl. Phys. Lett.* **2003**, *83*, 2052.
(22) Magnusson, M. H.; Deppert, K.; Malm, J. O. *J. Nanopart. Res.* **1999**, *1*, 243.
(23) Ohlsson, B. J.; Bjork, M. T.; Magnusson, M. H. *Appl. Phys. Lett.* **2001**, *79*, 3335.
(24) Thelander, C.; Bjork, M.; Larsson, T. M. W. *Solid State Commun.* **2004**, *131*, 573.
(25) Wang, D.; Wang, Q.; Javey, A. *Appl. Phys. Lett.* **2003**, *83*, 2432.
(26) Larsson, W.; Wagner, J. B.; Wallin, M. *Nanotechnology* **2007**, *18*.

NL0731062